Int. J. of Applied Mechanics and Engineering, 2022, vol.27, No.2, pp.115-123
DOI: 10.2478/ijame-2022-0023

COMPARISON OF THE RESULTS FOR CALCULATION OF VORTEX CURRENTS AFTER SUDDEN EXPANSION OF THE PIPE WITH DIFFERENT DIAMETERS

B.M. KHOLBOEV*, D.P. NAVRUZOV, D.S. ASRAKULOVA,
N.R. ENGALICHEVA and A.A. TUREMURATOVA
Plekhanov Russian University of Economics in Tashkent, 3 Shakhriabad, Tashkent 100164, UZBEKISTAN
E-mail: bakhodir.kholboev@gmail.com

In this work, a numerical study of a sharply expanding highly swirling flow is carried out using v2-f models based on the Comsol Multiphysics 5.6 software package and a two-fluid turbulence model. The results obtained are compared with known experimental data with different pipe diameters. The purpose of this work is to test the ability of models to describe anisotropic turbulence. It is shown that the two-fluid model is more suitable for studying such flows.

Key words: two-fluid turbulence model, sudden expansion, velocity fluctuation, intensity of fluctuations, gas resistance, quasi-periodic regime.

1. Introduction

The flow after a sudden expansion of the pipe is one of the most common cases of a detachable flow when winding sharp edges of bodies. The process is accompanied by significant changes in the speed and pressure in the separation zone. The flow and heat exchange down the flow disconnection section depend on the prehistory of flow development and the surface geometry in the region of the separation section. Sudden expansion of flow in pipes or channels is commonly used as a flame stabilizer in combustion chambers, for intensification of heat transfer processes and in many other technical devices. Separation is often a phenomenon that leads to negative consequences: an increase in gas resistance in pipelines, a decrease in speed, and so on. The presence of a recirculation flow in the separation zone has a significant effect on the intensity of momentum, heat, and mass transfer processes and determines the structure of the turbulent flow [1].

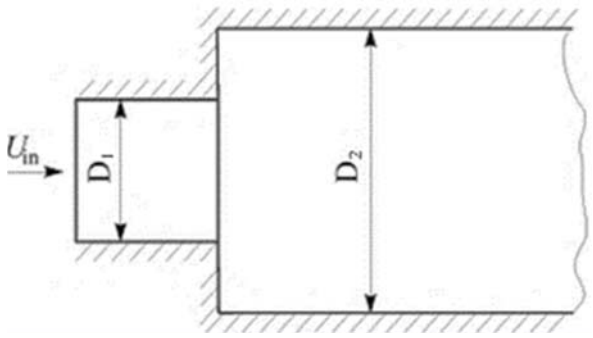

Fig.1. Pipe with sudden expansion.

* To whom correspondence should be addressed

Two-phase separated flows are frequently used in various technological applications. In addition to the above parameters, disperse phase influences the transport processes. Its impact increases with the growth of particle diameter and their concentration. The purpose of the work is to carry out a numerical study of the dispersion propagation in a turbulent flow after a sudden expansion of the pipe in the presence of heat exchange of the two-phase flow along the surface of the pipe wall and to compare the results of the two-phase flow liquid model with results of COMSOL software package.

As noted above, swirling flow problems are serious test problems for turbulence models. Therefore, as the next test task for verifying the new model, we considered the process of precession of a strongly swirling flow after a sudden expansion Fig.1. D_2 changes to $D_2 = 2D_1, 5D_1, 10D_1$.

2. Mathematical model

*The two-fluid mode*l:

Next there a mathematical model of turbulence based on the two fluid dynamics is considered. The system of equations for the turbulent flow has the following form [2]:

$$\begin{cases} \dfrac{\partial \rho}{\partial t} + \dfrac{\partial \rho U_i}{\partial x_i} = 0, \\ \dfrac{\partial \rho U_i}{\partial t} + \dfrac{\partial (\rho U_j U_i + \delta_{ij} p)}{\partial x_j} = \dfrac{\partial}{\partial x_j}\left(\Pi_{ij} - \rho \nu_i \nu_j\right), \\ \dfrac{\partial \rho v_i}{\partial t} + \rho U_j \dfrac{\partial v_i}{\partial x_j} = -\rho v_j \dfrac{\partial U_i}{\partial x_j} + \dfrac{\partial \pi'_{ij}}{\partial x_j} + F_{ri} + F_{\perp i}, \\ \Pi_{ij} = \mu\left(\dfrac{\partial U_i}{\partial x_j} + \dfrac{\partial U_j}{\partial x_i}\right), \qquad \pi'_{ij} = \rho \nu'_{\nu_i \nu_j}\left(\dfrac{\partial \nu_i}{\partial x_j} + \dfrac{\partial \nu_j}{\partial x_i}\right), \\ \nu'_{\nu_i \nu_j} = 3\nu + \left|\dfrac{\nu_i \nu_j}{def(U)}\right|, \qquad F_r = -\rho C_r \nu, \qquad F_\perp = 2\rho C_s rot U \times v. \end{cases} \tag{2.1}$$

It should be noted that π'_{ij} - is a tensor. Therefore, in the right part for a given tensor the summation for repeated indices is not performed.

We will study the problem in cylindrical coordinates. Longitudinal derivatives in diffusion terms are neglected. Then the system of Eq (2.1) in cylindrical coordinates will have the form:

$$\begin{cases} \dfrac{\partial V_z}{\partial z} + \dfrac{\partial r V_r}{r \partial r} = 0, \\ \dfrac{\partial V_z}{\partial t} + V_z \dfrac{\partial V_z}{\partial z} + V_r \dfrac{\partial V_z}{\partial r} + \dfrac{1}{\rho}\dfrac{\partial p}{\partial z} = \dfrac{1}{\mathrm{Re}}\left(\dfrac{\partial^2 V_z}{\partial r^2} + \dfrac{\partial V_z}{r \partial r}\right) - \dfrac{\partial r v_r v_z}{r \partial r}, \end{cases} \tag{2.2}$$

$$\begin{cases} \dfrac{\partial V_r}{\partial t}+V_z\dfrac{\partial V_r}{\partial z}+V_r\dfrac{\partial V_r}{\partial r}+\dfrac{1}{\rho}\dfrac{\partial p}{\partial r}=\dfrac{V_\varphi^2}{r}+\dfrac{1}{\mathrm{Re}}\left(\dfrac{\partial^2 V_r}{\partial r^2}+\dfrac{\partial V_r}{r\partial r}-\dfrac{V_r}{r^2}\right)-\dfrac{\partial r v_r v_r}{r\partial r}, \\ \dfrac{\partial V_\varphi}{\partial t}+V_z\dfrac{\partial V_\varphi}{\partial z}+V_r\dfrac{\partial V_\varphi}{\partial r}+\dfrac{V_r V_\varphi}{r}=\dfrac{1}{\mathrm{Re}}\left(\dfrac{\partial^2 V_\varphi}{\partial r^2}+\dfrac{\partial V_\varphi}{r\partial r}-\dfrac{V_\varphi}{r^2}\right)-\dfrac{\partial r^2 v_r v_\varphi}{r^2\partial r}, \\ \dfrac{\partial v_z}{\partial t}+V_z\dfrac{\partial v_z}{\partial z}+V_r\dfrac{\partial v_z}{\partial r}=-(1-2C_s)\dfrac{\partial V_z}{\partial r}v_r+\dfrac{1}{r}\dfrac{\partial}{\partial r}\left(r v'_{zr}\dfrac{\partial v_z}{\partial r}\right)-C_r v_z, \\ \dfrac{\partial v_r}{\partial t}+V_z\dfrac{\partial v_r}{\partial z}+V_r\dfrac{\partial v_r}{\partial r}=-2C_s\dfrac{\partial V_z}{\partial r}v_z-\left(2C_s\dfrac{\partial r V_\varphi}{r\partial r}-\dfrac{2V_\varphi}{r}\right)v_\varphi+ \\ +\dfrac{2}{r}\dfrac{\partial}{\partial r}\left(r v'_{rr}\dfrac{\partial v_r}{\partial r}\right)-2v'_{rr}\dfrac{v_r}{r^2}-C_r v_z, \\ \dfrac{\partial v_\varphi}{\partial t}+V_z\dfrac{\partial v_\varphi}{\partial z}+V_r\dfrac{\partial r v_\varphi}{r\partial r}=-(1-2C_s)\dfrac{\partial r V_\varphi}{r\partial r}v_r+\dfrac{1}{r^2}\dfrac{\partial}{\partial r}\left[r^2 v'_{\varphi r}\left(\dfrac{\partial v_\varphi}{\partial r}-\dfrac{v_\varphi}{r}\right)\right]-C_r v_\varphi. \end{cases} \tag{2.2cd}$$

To determine the molar viscosities, we use the relations:

$$v'_{zr}=3v+2\left|\frac{v_z v_r}{def(U)}\right|,$$

$$v'_{rr}=3v+2\left|\frac{v_r v_r}{def(U)}\right|,$$

$$def(U)=\sqrt{\left(\frac{\partial V_z}{\partial r}\right)^2+\left(\frac{\partial V_\phi}{\partial r}-\frac{V_\phi}{r}\right)^2}\ .$$

Solving the characteristic equation, we find the maximum root:

$$\lambda_{\max}=\sqrt{D},\ \text{if}\ D\geq 0,$$

$$\lambda_{\max}=0,\ \text{if}\ D\leq 0,$$

where

$$D=2C_s(1-2C_s)\left[\left(\frac{\partial r V_\varphi}{r\partial r}\right)^2+\left(\frac{\partial V_z}{\partial r}\right)^2\right]-\frac{2(1-2C_s)V_\varphi}{r}\frac{\partial r V_\varphi}{r\partial r}.$$

According to the formula:

$$C_r = C_1 \lambda_{\max} + C_2 \frac{|v_r|}{d},$$

here, d – is the nearest distance to the solid wall. The coefficients C_1, C_2 are the same as for the first task.

$v^2 - f$ turbulence model:

Near solid walls, the intensity of velocity fluctuations tangent to the wall is usually much higher than the intensity of fluctuations in the normal direction to the wall. In other words, velocity fluctuations are characterized by anisotropy. As we move away from the wall, the intensity of fluctuations in all directions becomes the same. Velocity fluctuations become similar or isotropic. The anisotropy of turbulent fluctuations in the boundary layer is described by the $v^2 - f$ turbulence model by introducing two additional equations, which are solved jointly with the equations for the kinetic energy of turbulence (k) and the rate of dissipation of kinetic energy (ε).

$$\begin{cases} (\bigcup \cdot \nabla) k = \nabla \left[\left(v + \frac{v_i}{\sigma_k} \right) \nabla k \right] + P - \varepsilon, \\ (\bigcup \cdot \nabla) \varepsilon = \nabla \left[\left(v + \frac{v_t}{\sigma_\varepsilon} \right) \nabla \varepsilon \right] + \frac{1}{\tau} \left[C'_{\varepsilon 1} (\zeta, \alpha) P_k - C'_{\varepsilon 2} (k, \varepsilon, \alpha) \varepsilon \right], \\ (\bigcup \cdot \nabla) \zeta = \nabla \left[\left(v + \frac{v_t}{\sigma_\zeta} \right) \nabla \zeta \right] + \frac{2}{k} \left[\alpha^3 v + \frac{v_t}{\sigma_\zeta} \right] \nabla k \nabla \zeta + \left(1 - \alpha^3 \right) f_w + \alpha^3 f_h - \frac{\zeta}{k} P_k. \end{cases} \quad (2.3)$$

Turbulent eddy viscosity is calculated is used. Other coefficients and functions were presented in the article [3].

3. Numerical method

To ensure stability in solving the Eq.(2.2) of the system, the convective members use a differential scheme against the second-order flow of accuracy by the control volume method. And, the implicit central difference for the diffusion terms. The relationship between the velocity and pressure fields for an incompressible fluid was implemented using the SIMPLEC procedure [4]. After the formation of a quasi-periodic regime, the non-stationary fields were averaged.

At the input, an experimental velocity profile was set, measured for the cross section $z = -5D$ corresponding to the input location of the calculated area. At the output $z = 5D$, "soft" conditions were set. The stream had the following input parameters:

$$\mathrm{Re} = \frac{DU_{in}}{v} = 30000, \qquad S = \frac{\int_0^R V_{0\varphi} V_{0z} r^2 dr}{R \int_0^R V_z^2 r dr} = 0.6,$$

$$v_\varphi = 0.2U_{im}, \qquad v_z = 0.2U_{in}, \qquad v_r = 0.05U_{in},$$

here, Re - is the Reynolds number, S - is a the parameter that determines the extent of the inlet flow, and U_{in} - is the maximum axial velocity at the inlet. For calculations, a 100×100 grid was used. Equations in a dimensionless

form were given by correlating all velocities to U_{in}, and spatial scales to the diameter of a small tube. Integration over time was carried out with a dimensionless step $\Delta t = 0.001$. The entry conditions are as follows:

$$V_\varphi = V_{0\varphi}\left(1 - \frac{0.1z}{D}\right),\ V_z = V_{0z},\ V_r = 0,\ \text{if } z > 0 \text{ and } r < 0.5D,$$

$$V_\phi = V_z = V_r = 0,\ \text{if } z > 0 \text{ and } r > 0.5D.$$

4. Results and discussions

In Figs 1-4, the solid lines represent the numerical results which are compared to results obtained by numerical methods most commonly used during the last two decades to solve different models [10, 11, 12].

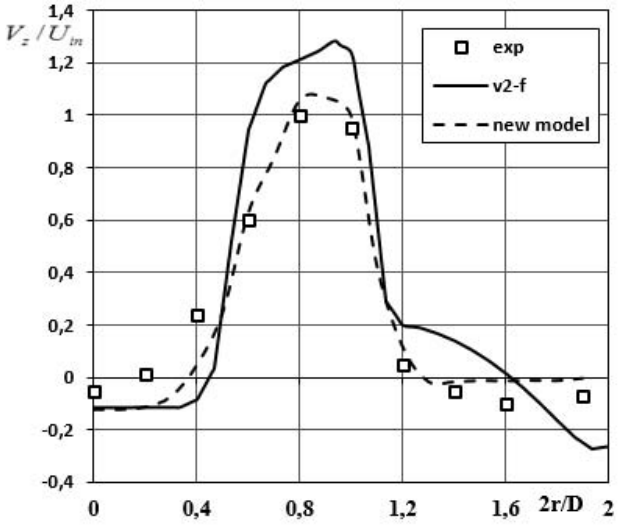

Fig.1. Axial speed profile.

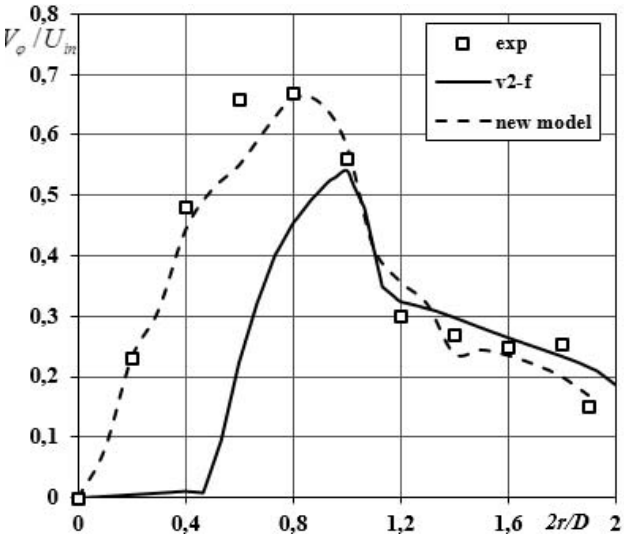

Fig.2. Tangential velocity profile.

Dots depict experimental data obtained in [5]. Here, all spatial scales are related to the diameter of the inlet pipe. Figures 1 and 2 show the profiles of the axial and tangential flow velocities in the section $x = 0.2$, respectively. Similar graphs are shown in Figs 3 and 4 for $x = 0.5$.

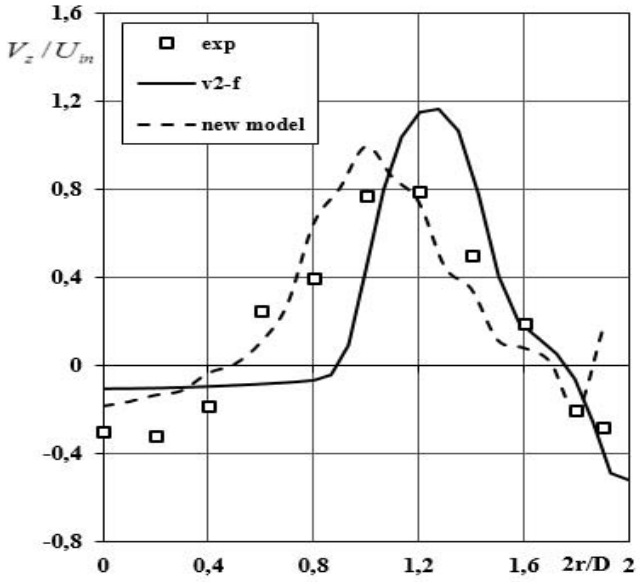

Fig.3. Axial speed profile.

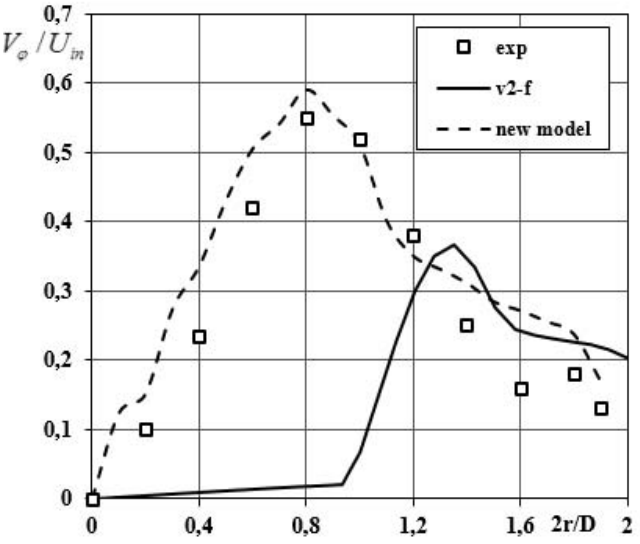

Fig.4. Tangential velocity profile.

In Figures 5-8, the solid lines represent the numerical results. Here, the second pipe diameter is five times larger than the first pipe. Figs 5 and 6 show the profiles of the axial and tangential flow velocities in the section $x = 0.2$, respectively. Similar graphs are shown in Figs 7 and 8 for $x = 0.5$.

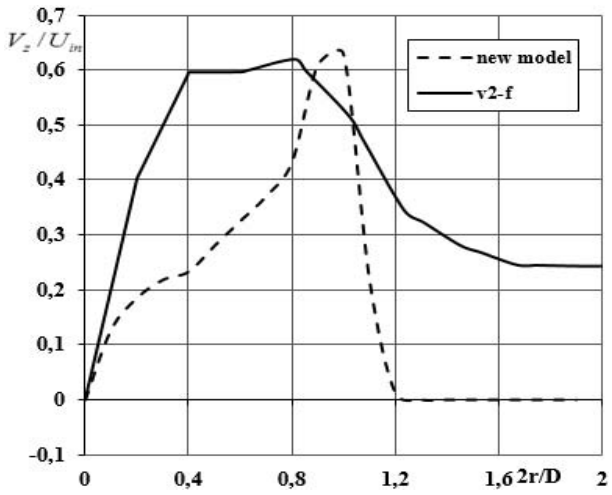

Fig.5. Axial speed profile.

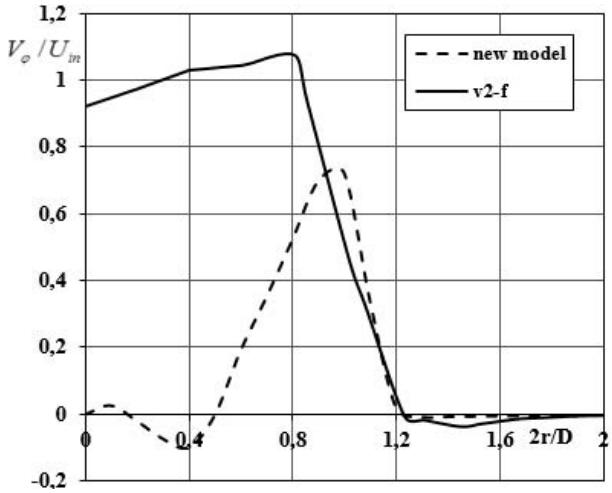

Fig.6. Axial speed profile.

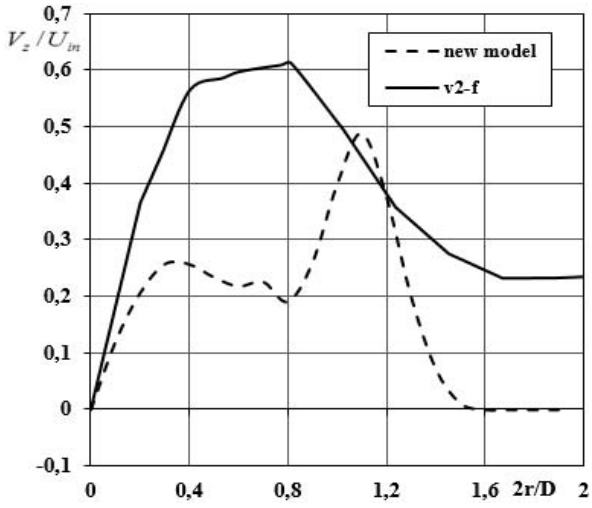

Fig.7. Axial speed profile.

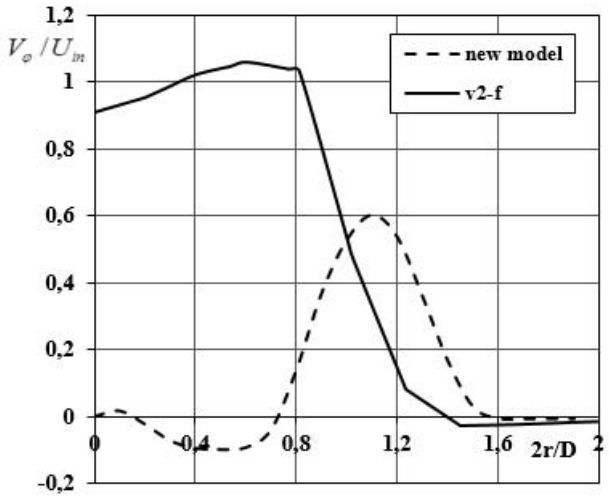

Fig.8. Axial speed profile.

5. Conclusion

The paper shows the possibility of modeling a vortex flow after a sudden expansion using a new model. Mathematical modeling was carried out on the basis of the dynamics of two fluids. The calibration and verification of the new model was carried out on known tasks that have been well investigated experimentally. Despite the fact that the nature of turbulence in these problems is different, the new model quantitatively describes these complex flows well.

Acknowledgements

This work was supported by the Ministry of Innovative Development of the Republic of Uzbekistan (research project no.21071166), supported by the Government of Republic of Uzbekistan.

Nomenclature

D_1 – first pipe diameter

D_2 – second pipe diameter

v'_{zr}, v'_{zr} – molar viscosities

λ_{max} – maximum root of the characteristic equation

d – closest distance to solid wall

C_1, C_2 – coefficients

Re – Reynolds number

S – degree twist

U_{in} – maximum axial input speed

References

[1] Abramovich G.N. (1984): *Theory of Turbulent Jets*.– Moscow, "Nauka", p.718.

[2] Malikov Z.M. (2020): *Mathematical model of turbulence based on the dynamics of two fluids.*– Applied Mathematic Modeling, No.82, pp.409-436.

[3] Smirnov P.E. (2006): *Testing the v2-f-model of turbulence in the calculation of flow and heat transfer in a channel with a sudden expansion.*– Inzhenerno-Fizicheskij Zhurnal, vol.79, No.4, p.38.

[4] Patankar S.V. (1980): *Numerical Heat Transfer and Fluid Flow*.– Taylor and Francis, ISBN 978-0-89116-522-4, p.214.

[5] Dellenback P.A., Metzger D.R. and Neitzel G.P. (1988): *Measurements in turbulent swirling flow through an abrupt expansion*.– AIAA J., vol.26, No.6, pp.669-681.

[6] Anderson D.A., Tannehill J.C. and Pletcher R.H. (1990): *Computational fluid mechanics and heat transfer*.– M.: Mir, vol.1, pp-384, vol.2, pp-392.

[7] Mises R.V. (1927): *Remarks on hydrodynamics.*– NASA Transl. into english from Z. Angew. Math. Mech. (Berlin), vol.7, pp. 425-431.

[8] Bradshaw P., Ferriss D.H. and Atwell N.P. (1967): C*alculation of boundary layer development using the turbulent energy equation*.– J. Fluid Mech., vol.28, pp.593-616.

[9] Spalart, P.R. and Allmaras, S.R. (1992): *A One-Equation Turbulence Model for Aerodynamics Flows.*– Boeing Commercial Airplane Group, Seattle, Washington.

[10] Volk B.L., Lagoudas D.C., Chen Y.C. and Whitley K.S. (2010): *Analysis of the finite deformation response of shape memory polymers: I. Thermomechanical characterization*.– Smart Materials and Structures, vol.19, No.7, p.10, DOI: 10.1088/0964-1726/19/7/075005

[11] Ratajczak M., Ptak M., Chybowski L., Gawdzińska K. and Będziński R. (2019): *Material and structural modeling aspects of brain tissue deformation under dynamic loads*.– Materials, MDPI, vol.12, No.2, Article number 271, p.13, doi: 10.3390/ma120271.

[12] Reparaz J.S., Pereira da Silva K., Romero A.H., Serrano J., Wagner M.R., Callsen G., Choi S.J., Speck J.S. and Goñi A.R. (2018): *Comparative study of the pressure dependence of optical-phonon transverse-effective charges and linewidths in wurtzite*.– In N. Phys. Rev. B, vol.98, Article number 165204, DOI: https://doi.org/10.1103/PhysRevB.98.165204.

Received: February 2, 2022
Revised: May 19, 2022